Frequency Domain Total Least Squares Estimator of Time-Varying Systems

John Lataire and Rik Pintelon
Vrije Universiteit Brussel - dept. ELEC, Pleinlaan 2, 1050 Brussels

Abstract— **An identification procedure for linear continuous-time, time-varying systems is presented. The model considered is an ordinary differential equation whose coefficients are polynomials in time. The model equation is evaluated in the frequency domain (thus allowing a simple selection of the frequency band of interest) from sampled, finite length records of the input and output signals. The time-frequency transformations are performed using the Discrete Fourier Transform and its inverse. The leakage and alias errors (due to the non-periodicity of the system's response) are shown to be easily captured by adding a polynomial to the model equation. The identification procedure is formulated as a total least squares estimation problem. The estimator is illustrated on a simulation example.**

I. Introduction

Time-varying systems are appearing in many engineering applications. Consider for instance the study of the resonance frequencies and the associated damping ratios of the wings of a plane. These are functions of the flight speed and height and, thus, are time-varying while flying [1]. As a second example, consider the impedance of a metal undergoing an electro-chemical reaction, such as pitting corrosion [2]. Since the number and size of the pits evolve in time, this is a time-varying system too. From a practical point of view, it could be assumed that the time variation can either be frozen (by allowing the plane to fly at a constant speed and height) or is much slower than the typical time constants of the dynamics of the system, such that identification techniques for time invariant systems can be acquired. Time-varying models, however, offer the possibility of actually modelling the time evolution of the dynamics. Advantages include i) a natural way of interpolating between various 'frozen' states of the system, and ii) modelling by means of long measured records (such as to cover a wide range of the time variation at once).

Most earlier work on time-varying systems focused on identifying discrete time systems and working in the time domain [3], [4], [5]. Contrary to that, frequency domain methods are used in this paper. These have proven their usefulness in system identification for the efficient selection of a desired frequency band of interest and the immediate identification of continuous-time, linear, time invariant models from sampled data in a band-limited measurement setup [6], [7].

An advantage of time domain methods is that they simplify the immediate identification of the model as being dependent on an external 'scheduling' parameter [3], [4] (e.g. the flight height/speed in the example with the plane). In the present work, the dependence on scheduling parameters is not taken into account, resulting in possibly less rich models. However, the simplicity of implementing the proposed estimators relieves (at least partly) that burden. Moreover, having identified a time-varying model, and combining this with the measured scheduling parameters, a parameter varying model could be obtained in a second step.

In this work, the system model considered is a linear ordinary differential equation with time dependent coefficients. The latter are assumed to be described by polynomials in time. It will be shown how the required Fourier transforms of the signals can be approximated by the discrete Fourier transforms of their sampled counterpart, provided that half the sampling frequency exceeds the excited frequency band. The total least squares estimator is constructed. A re-parametrisation is performed to obtain an improved robustness w.r.t. disturbing noise.

This paper is organised as follows. Section II defines the system model considered, both in the time and in the frequency domain, and highlights the practical issues of windowing and sampling the signals. Section III discusses the origin of the leakage and alias errors for the given model class, and shows how they can be captured during the identification. A noise robust Total Least Squares estimator is constructed in Section IV. The proposed method is illustrated on simulation data in Section V, and Section VI draws the conclusions.

II. Model Equation

A. Time domain model equation

The considered systems are assumed to fulfil a linear ordinary differential equation (ODE) with time-varying coefficients:

$$\sum_{n=0}^{N_\alpha} \alpha_n(t) \frac{d^n y(t)}{dt^n} = \sum_{n=0}^{N_\beta} \beta_n(t) \frac{d^n u(t)}{dt^n} \tag{1}$$

where $u(t)$ and $y(t)$ are the input and output signals respectively. The time-varying coefficients $\alpha_n(t)$ and $\beta_n(t)$ are assumed to be real valued polynomials in t:

This work was supported in part by the Fund for Scientific Research (FWO-Vlaanderen), by the Flemish Government (Methusalem Fund, METH1), and by the Belgian Federal Government (IUAP VI/4). J. Lataire's work was supported by the Research Foundation – Flanders (FWO) under a Ph. D. fellowship. E-mail: jlataire@vub.ac.be, phone: +32 (0)2 629 29 42

ISBN 978-963-311-370-7

$$\alpha_n(t) = \sum_{p=0}^{N_p} \alpha_{n,p} t^p \qquad \beta_n(t) = \sum_{p=0}^{N_p} \beta_{n,p} t^p \tag{2}$$

Remark 2.1: As polynomials have the property to be unbounded for $t \to \pm\infty$, system (1) is most likely to be unstable if not restricted to a limited time window. In the remainder, it will be assumed that (1) and (2) are (at least) valid in the time interval $t \in [0, T]$.

A more general parametrisation of system (1) is

$$\sum_{n=0}^{N_\alpha} \sum_{p=0}^{N_p} \tilde{\alpha}_{n,p} b_p(t) \Psi_n\{y(t)\} = \sum_{n=0}^{N_\beta} \sum_{p=0}^{N_p} \tilde{\beta}_{n,p} b_p(t) \Psi_n\{u(t)\} \tag{3}$$

where $b_p(t)$ is a polynomial in t and $\Psi_n\{x\}$ is a polynomial derivative operator on x. If the sets $\{b_0(t), \ldots, b_p(t)\}$ and $\{\Psi_0, \ldots, \Psi_n\}$ form bases for polynomials in t of order p, and polynomial derivative operators of order n respectively, then a linear relationship exists between $\tilde{\alpha}_{n,p}$ (resp. $\tilde{\beta}_{n,p}$) and the parameters $\alpha_{n,p}$ (resp. $\beta_{n,p}$) of (1). As a consequence, (1) and (3) are equivalent. For simplicity, the derivation for the computation of the model equation will be performed for (1). In Section IV-A, it will be shown how a good choice of $b_p(t)$ and Ψ_n allows for a better robustness of the total least squares estimator to noise.

The identification problem consists of estimating the system parameters, namely the coefficients $\alpha_{n,p}$ and $\beta_{n,p}$ (or equivalently $\tilde{\alpha}_{n,p}$ and $\tilde{\beta}_{n,p}$) from measurements of the input and output signals. The model can be generalised to allow piecewise polynomial variations. Additional (linear) constraints are then applied to the system parameters to ensure smooth transitions between time pieces, as was briefly discussed in [8]. As such, arbitrary time variations can be modelled.

Define, for further use, the equivalent instantaneous system at a constant time instant t^* as the time invariant system described by

$$\sum_{n=0}^{N_\alpha} \alpha_n(t^*) \frac{d^n y(t)}{dt^n} = \sum_{n=0}^{N_\beta} \beta_n(t^*) \frac{d^n u(t)}{dt^n} \tag{4}$$

B. Frequency domain model equation

The differential equation (1) can be rewritten in the frequency domain by applying the Fourier transform to its both sides.

$$\mathcal{F}\left\{\sum_{n=0}^{N_\alpha} \alpha_n(t) \frac{d^n y(t)}{dt^n}\right\}\Bigg|_{\omega_k} = \mathcal{F}\left\{\sum_{n=0}^{N_\beta} \beta_n(t) \frac{d^n u(t)}{dt^n}\right\}\Bigg|_{\omega_k} \tag{5}$$

where $\mathcal{F}\{x\}$ is the Fourier transform of x. As noted, these Fourier transforms are considered at a discrete set of angular frequencies $\omega_k = \frac{2\pi k}{T}$, $k \in \mathbb{K} \subset [0, N/2] \cap \mathbb{N}$. Thus, ω_k is the angular frequency corresponding to the kth bin of the Discrete Fourier Transform (DFT) of a sampled time domain signal of length T. $\mathbb{K}$ is a set of considered frequency indices, determining the frequency band(s) of interest. The latter is, in the same frame of mind as Remark 2.1, determined from the application area of the system under test. One should ensure that the frequencies corresponding to the indices in $\mathbb{K}$ yield the frequency band in which the system is (usually) operated.

Equation (5) being linear in the system parameters, it can be rewritten as

$$\mathbf{K}\theta = 0, \quad \text{with } \mathbf{K} = \begin{bmatrix} \mathbf{K}_Y & -\mathbf{K}_U \end{bmatrix} \tag{6}$$

with θ the column vector stacking all the system parameters

$$\theta = \begin{bmatrix} \cdots & \alpha_{n,p} & \cdots & \beta_{n,p} & \cdots \end{bmatrix}^T, \tag{7}$$

and $\mathbf{K}_{Y/U} \in \mathbb{C}^{F \times [(N_{\alpha/\beta}+1)(N_p+1)]}$, with F the number of elements in $\mathbb{K}$. $\mathbf{K}$ will be referred to as the regression matrix. The column of $\mathbf{K}_Y$ (resp. $\mathbf{K}_U$) corresponding to $\alpha_{n,p}$ (resp. $\beta_{n,p}$) is given by

$$\mathcal{F}\left\{t^p \frac{d^n y(t)}{dt^n}\right\}\Bigg|_{\omega=\omega_k}, \quad \left(\text{resp. } \mathcal{F}\left\{t^p \frac{d^n u(t)}{dt^n}\right\}\Bigg|_{\omega=\omega_k}\right). \tag{8}$$

Some practical aspects for computing $\mathbf{K}$ arise:

- The Fourier transform is meant to be applied to an infinitely long signal, which is certainly not available. The effect of restricting (8) to a finite record length is taken into account in Section III-A (and is in accordance with Remark 2.1).
- The continuous time signals are available as sampled series. The possible aliasing errors will be discussed in Section III-B.

It will be shown that both errors can be approximated very well by a polynomial function of the frequency.

III. Capturing transient and alias errors

A. Windowing the signals

Consider the windowed signal $x(t)$ (s.t. $x(t) = 0$ for $t < 0$ or $t > T$) and its Laplace transform $X(s)$, and compute the following:

$$\begin{aligned} \mathcal{L}\left\{t^p \frac{d^n x(t)}{dt^n}\right\} &= (-1)^p \frac{d^p}{ds^p}\left[s^n X(s) + I_{x,n}(s)\right] \\ &= (-1)^p \frac{d^p}{ds^p} s^n X(s) + I_{x,n}^{(p)}(s) \\ &= \mathcal{L}\left\{t^p \mathcal{L}^{-1}\left\{s^n X(s)\right\}\right\} + I_{x,n}^{(p)}(s) \end{aligned} \tag{9}$$

where the first equality is proven in Appendix VII-A. $X(s) = \mathcal{L}\{x(t)\}$ denotes a Laplace transform (s is the Laplace variable) and $I_{x,n}^{(p)}(s)$ is a polynomial of order less than or equal to $n-1$ when evaluated at the DFT frequencies.

Note that expression (9) chooses the most convenient domain (time or frequency) to perform the operations on the signals (a multiplication is preferred to a derivative), provided that the Laplace transform (and its inverse) can be computed.

Applying expression (9) to the ODE (1) for the windowed input and output signals $u_T(t)$ and $y_T(t)$ yields

$$\sum_{n=0}^{N_\alpha}\sum_{p=0}^{N_p}\alpha_{n,p}\mathcal{L}\left\{t^p\mathcal{L}^{-1}\left\{s^n\mathcal{L}\{y_T(t)\}\right\}\right\} \tag{10}$$
$$=\sum_{n=0}^{N_\beta}\sum_{p=0}^{N_p}\beta_{n,p}\mathcal{L}\left\{t^p\mathcal{L}^{-1}\left\{s^n\mathcal{L}\{u_T(t)\}\right\}\right\}+I(s),$$

with $\begin{cases} u_T(t)=u(t),\ y_T(t)=y(t) & \text{for } 0\le t\le T \\ u_T(t)=y_T(t)=0 & \text{for } t<0\vee t>T \end{cases}$

It reveals that $u_T(t)$ and $y_T(t)$ fulfil a very similar ODE as the original one: when evaluated at $s_k=j\omega_k$ the only difference is the polynomial $I(s_k)$ of order $\max(N_\alpha,N_\beta)-1$, which will be referred to as the "transient term". Similarly as for (6), when sampled at s_k, (10) is rewritten as

$$\mathbf{K}_T\theta_T=0,\quad \text{with} \tag{11}$$
$$\mathbf{K}_T=\begin{bmatrix}\mathbf{K}_{Y_T} & -\mathbf{K}_{U_T} & 1 & s_k & \cdots & s_k^{\max(N_\alpha,N_\beta)-1}\end{bmatrix},$$

θ_T is obtained by appending the coefficients of $I(s_k)$ to θ. The column of $\mathbf{K}_{Y_T}$ (resp. $\mathbf{K}_{U_T}$) corresponding to $\alpha_{n,p}$ (resp. $\beta_{n,p}$) is given by

$$\mathcal{L}\left\{t^p\mathcal{L}^{-1}\left\{s^n\mathcal{L}\{y_T(t)\}\right\}\right\}\Big|_{s=j\omega_k}, \tag{12}$$
$$\left(\text{resp. }\ \mathcal{L}\left\{t^p\mathcal{L}^{-1}\left\{s^n\mathcal{L}\{u_T(t)\}\right\}\right\}\Big|_{s=j\omega_k}\right).$$

Remark 3.1: From Appendix VII-A and (9) it follows that the coefficients of the polynomial $I(s_k)$ are functions of the input and output signals and their derivatives at time instants 0 and T. Their exact values are usually of no practical importance since i) after identification of $\alpha_{n,p}$ and $\beta_{n,p}$ they are reconstructible from the system equation and the identified parameters, ii) they are hardly distinguishable from aliasing errors, as explained in Section III-B.
However, the inclusion of $I(s_k)$ in the estimation algorithm will be required to avoid modelling errors.

B. Approximation using sampled signals

In practical situations, the signals are available as sampled data. The required Fourier transforms can be approximated by their DFT (Discrete Fourier Transform):

$$X_T(j\omega_k)\equiv\int_0^T x(t)e^{-j\omega_k t}\mathrm{d}t\approx T_s\sum_{t_d=0}^{N-1}x(t_dT_s)e^{-j\omega_k t_dT_s}$$
$$\approx T_s\mathtt{DFT}\{x_T(t_dT_s)\}\equiv T_sX_T(k) \tag{13}$$

where $T_s=\frac{1}{f_s}$ is the sample period, $N=Tf_s$ is the number of sampled points in the record, and t_d denotes the sample time indices. Define also the inverse DFT operation.

$$\mathtt{iDFT}\{X_T(k)\}|_{t_d}\equiv\frac{1}{N}\sum_{k=0}^{N-1}X_T(k)e^{j\omega_k t_dT_s}$$

The Fourier transform and its inverse are thus approximated by the left Riemann sum of their corresponding integral. It is well known [9] that

$$\mathtt{DFT}\{x(t_dT_s)\}=\frac{1}{T_s}\sum_{k'=-\infty}^{\infty}X(j\omega_{k-k'f_s}), \tag{14}$$

such that the actual output spectrum is repeated around each multiple of f_s.

Using the DFT of the sampled signals for computing (12) means that the following approximation is made:

$$\mathcal{L}\left\{t^p\mathcal{L}^{-1}\left\{s^n\mathcal{L}\{x_T(t)\}\right\}\right\}\Big|_{s=j\omega_k} \tag{15}$$
$$\approx T_s\mathtt{DFT}\{(t_dT_s)^p\mathtt{iDFT}\{(s_k^n)\mathtt{DFT}\{x_T(t_dT_s)\}\}\}$$

The consequences of this approximation are graphically illustrated by Figures 1 to 4. The reasoning is as follows.

Consider $x(t)$ to be periodic (period $T=NT_s$) and band-limited to $]-\frac{f_s}{2},\frac{f_s}{2}[$ (that is $X=0$ outside that interval). The spectrum of $x(t)$ is discrete, as illustrated in Fig. 1. After windowing we have that:

$$\mathtt{DFT}\{x_T(t_dT_s)\}|_k=\frac{1}{T_s}X_T(j\omega_k). \tag{16}$$

That is, the DFT of a periodic, windowed (rectangular), sampled, band-limited signal is exactly equal to its Fourier transform at the Fourier frequencies $\omega_k=\frac{2\pi k}{T}$ if the period of the signal (or an integer multiple of it) coincides with the length of the window.

The spectrum $s^nX_T(s)|_{s=j\omega_k}$ is given in Fig. 2. Being still band-limited and time-periodic, $\mathcal{L}^{-1}\{s^nX_T(s)\}$ is exactly computed by using the iDFT. The multiplication by t^p yields

$$t^p\mathcal{L}^{-1}\{s^nX_T(s)\}\Big|_{t=t_dT_s} \tag{17}$$
$$=(t_dT_s)^p\mathtt{iDFT}\{s_k^nX_T(k)\},$$

which is exact at the sample points. The left hand side of this equation is a time domain multiplication which, in the frequency domain corresponds to a convolution. That is, the spectrum of the monomial t^p is convolved with a discrete spectrum, which is graphically understood as follows. The spectrum of the monomial is scaled, phase shifted, and pasted around each excited frequency of the periodic signal's spectrum. Since the spectrum of the monomial t^p is shaped like a skirt (it actually is a hyperbola, as proven in Appendix VII-B), the result of the convolution (shown in Fig. 3) consists of adjacent skirt-like contributions, each centred around the excited frequencies.

The spectrum in Fig. 3 clearly extends beyond the excited frequency band of $x(t)$. This causes alias errors when time-sampled. As given by (14) and illustrated in Fig. 4 the spectrum is repeated around multiples of the sampling frequency (the first repetition is shown in the figure). Consider the hyperbola centred around the first excited frequency in the repeated spectrum (explicitly drawn with a black full line in the figure). This hyperbola causes alias in the frequency

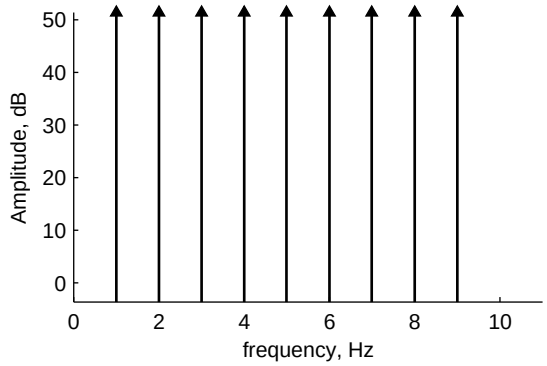

Fig. 1. Spectrum of a band-limited and periodic signal x.

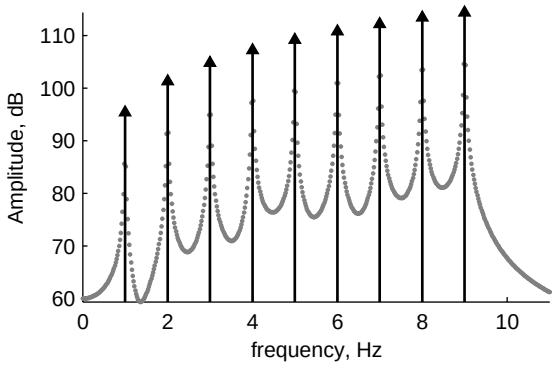

Fig. 3. Spectrum of the signal $t\frac{dx}{dt}$, after windowing (rectangular)

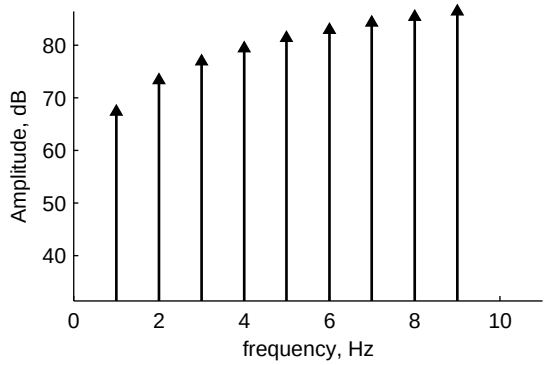

Fig. 2. Spectrum of $\frac{dx}{dt}$.

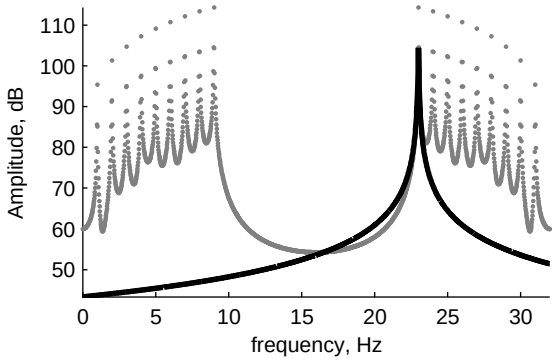

Fig. 4. Spectrum of sampled and windowed signal $t\frac{dx}{dt}$, zoomed out, with first repetition of the spectrum around the sample frequency. The first hyperbola in the repeated spectrum is shown explicitly (black full line).

band of interest. This error, however, is smooth, which has the major advantage that it can be captured by a polynomial in s_k. As such, the alias error can be distinguished from the actual signal.

Note that the response of a time-varying system is neither periodic, nor band-limited. It intrinsically causes aliasing. However, if the excitation is band-limited, the resulting response is also found to be smooth beyond the Nyquist frequency. A similar reasoning as for periodic, band-limited signals shows that the aliasing errors made when computing the regression matrices can also be captured by a polynomial [10].

The consequence of this discussion is that the sampled signals fulfil the following equation:

$$\sum_{n,p}\alpha_{n,p}\mathtt{DFT}\{(t_dT_s)^p\mathtt{iDFT}\{(j\omega_k)^n\mathtt{DFT}\{y_T(t_dT_s)\}\}\} \quad (18)$$
$$=\sum_{n,p}\beta_{n,p}\mathtt{DFT}\{(t_dT_s)^p\mathtt{iDFT}\{(j\omega_k)^n\mathtt{DFT}\{u_T(t_dT_s)\}\}\}$$
$$+\delta_a(k)+I(s_k),$$

where the summations over n and p are the same as in (10). $\delta_a(k)$ is the total aliasing error. As such, and unless the signals are highly oversampled, δ_a is undistinguishable from $I(s_k)$, introduced in (10). This is permitted, as pointed out in Remark 3.1.

To conclude, both the transient term and the aliasing errors are captured by the polynomial's base, appended to the regression matrix in (11). It might however be required to use an order higher than $\max(N_\alpha, N_\beta)-1$. The columns of the regression matrices $\mathbf{K}_{U_T}$ and $\mathbf{K}_{Y_T}$ are computed as the right hand side of (15) by replacing x by u_T and y_T.

IV. Total Least Squares estimator

Measured signals are corrupted by noise and, thus, do not perfectly fulfil the system equation (even if the measured system is in the model set). The Total Least Squares (TLS) estimator finds the set of parameters for which it holds that

$$\mathbf{K}_{T,m}\hat{\theta}_{\text{TLS}} \approx 0 \quad \text{subject to } \|\hat{\theta}_{\text{TLS}}\|_2 = 1. \quad (19)$$

The approximation is understood in least squares sense. $\mathbf{K}_{T,m}$ is the regression matrix defined in (11), computed using the measured signals. $\hat{\theta}_{\text{TLS}}$ is the TLS estimate of θ_T. It is obtained as the right singular vector corresponding to the smallest singular value of $\mathbf{K}_{T,m}$, as described for instance in [11].

A. Using Legendre basis functions for the TLS estimator

As suggested by (3), a re-parametrisation of the system can be performed. Replacing s^n by $\Psi_n(s)$ (an nth order polynomial in s), and t^p by $b_p(t)$ (a pth order polynomial in

t) in (10) yields just another description of the same system. In addition, the computation of the regression matrix is completely analogous as explained as for simple monomials.

The robustness to disturbing noise of the TLS estimator was experienced to drastically improve when $b_p(t)$ and $\Psi_n(s)$ were set equal to (scaled and shifted) Legendre polynomials. The intuitive explanation is that, contrary to simple monomials s^n and t^p which can get extremely high for growing values of s and t, the Legendre polynomial's energy is nicely spread over the considered (time or frequency) domain. This yields a more homogeneous weight of the residuals in the cost function. Note that, since Legendre polynomials are known to form a basis for polynomials, the resulting model set is exactly the same as the one obtained when using simple monomials.

Consider the nth order Legendre polynomial $P_n(x)$ and define the time domain basis functions as $b_p(t) = P_p\left(\frac{2t}{T} - 1\right)$. The frequency domain basis functions are defined as follows:

$$\Psi_n(j\omega) = \begin{cases} jP_n\left(\frac{\omega}{\omega_{\max}}\right) & \text{for } n \text{ odd} \\ P_n\left(\frac{\omega}{\omega_{\max}}\right) & \text{for } n \text{ even} \end{cases} \tag{20}$$

where $\omega_{\max}$ is the upper bound of the frequency band of interest. Knowing that the polynomial P_n has odd order for n odd and even order for n even, it is simple to conclude that $\Psi_n(-j\omega) = \overline{\Psi_n(j\omega)}$, as required for real systems. The improvement when using Legendre basis functions will be illustrated on a simulation example in Section V-B.

V. Simulation results

A. Noiseless case

The TLS estimator was applied to simulation data of the system whose instantaneous poles and zeroes (which are the poles and zeros of the instantaneous system (4)) evolved as shown in Fig. 5. It was simulated using the ODE solver 'ODE45' from Matlab®. The sampling frequency was $f_s = 2048Hz$. The frequency band $[0, 200]$Hz was excited.

The instantaneous FRF of the system at various time instants is given by the grey shaded lines in Fig. 6. The RMS error (over the instantaneous times) for different cases (labelled **A**, **B**, **C** and **D**) are given by the grey dashed lines:

- **A** The regression matrix was computed from sampled data. No additional polynomial was, however, estimated (thus not taking into account the transient and alias errors). The error clearly lies significantly higher than in the other cases.
- **B** An additional polynomial was estimated of order $N_{\text{tr}} = \max(N_\alpha, N_\beta) - 1 = 3$ (which is the theoretic value if no alias errors would be present). An impressive decrease in the error of more than 30dB is observed.
- **C** Again, $N_{\text{tr}} = 3$ was used. The sampling frequency was halved, yielding a slight increase of the alias error, which is seen also in the estimation error.

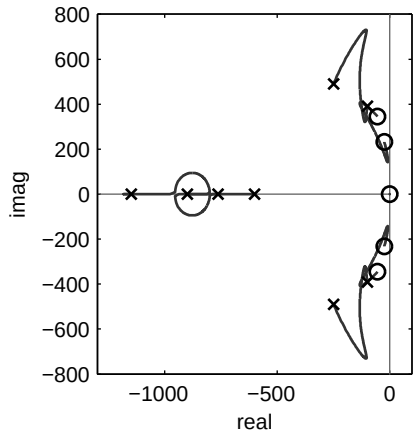

Fig. 5. Evolution of the instantaneous poles (x) and zeroes (o) of the simulated system.

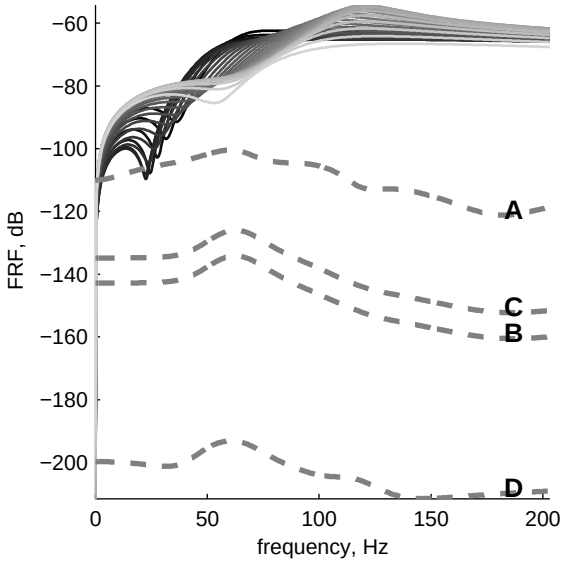

Fig. 6. Noiseless case: Evolution of the amplitude of the actual instantaneous FRF (gray shaded lines) of the simulated system. Grey dashed lines: RMS errors over all time instants of the estimated instantaneous FRFs.

- **D** The estimation error due to alias can be suppressed further by increasing N_{tr}. It was set to 7 in the figure. The RMS error now lies about 120dB below the estimate.

The decrease of the estimation error for an increasing order of the estimated transient term clearly motivates the need of including the latter in the estimation procedure.

B. Noisy Case

The improvement of the TLS estimator when using Legendre polynomials is illustrated on the same system as in Section V-A. The in- and output signals were corrupted by coloured noise s.t. the signal-to-noise ratio (SNR) was 28 dB. The results are shown in Fig. 7. The instantaneous FRFs are again given as a reference (full grey shaded lines). The errors

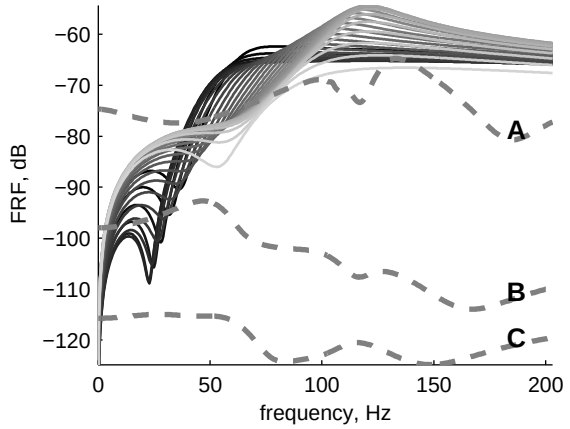

Fig. 7. Noisy case, same notational conventions as in Fig. 6.

(grey dashed lines) are discussed for three different cases:

- **A** Monomials in s and in t are used as time and frequency domain basis functions. The RMS error is of the same order of magnitude as the estimate itself.
- **B** Legendre polynomials are used as time and frequency domain basis functions. A tremendous decrease in the error is observed. Note that no noise information was used for performing this estimation.
- **C** A weighted nonlinear least squares was used, which applied a frequency domain weight to the rows of the regression matrix. This estimator was discussed in [10] and required information on the disturbing noise. A significant decrease of the RMS error is again observed.

From these results it is clear that, if no noise information is available, the choice of the basis functions plays an important role in the robustness of the TLS estimator w.r.t. disturbances. When available, noise information can significantly improve an estimator's performance.

VI. Conclusions

A frequency domain, Total Least squares estimator for continuous-time, time-varying systems was set up. The sampled continuous-time signals could be directly processed by very fast algorithms to obtain the required regression matrix. The transient (due to the non-periodicity of the response) and aliasing (due to the fact that the basis functions chosen were not band-limited) errors were shown to be well captured by additional polynomials in the frequency variable. The TLS estimator was shown to gain in robustness by a judicious choice of the basis functions. A qualitative motivation was given for choosing Legendre polynomials. The estimator was successfully illustrated on simulation data.

References

[1] A. Fujimori and L. Ljung, "Parameter estimation of polytopic models for a linear parameter varying aircraft system," *Transactions of the Japan Society for Aeronautical and Space Sciences*, vol. 49 (165), pp. 129–136, Nov. 2006.

[2] E. Van Gheem, J. Vereecken, J. Schoukens, R. Pintelon, P. Guillaume, P. Verboven, and L. Pauwels, "Instantaneous impedance measurements on aluminium using a schroeder multisine excitation signal," *Electrochimica Acta*, vol. 49, no. 17–18, pp. 2919–2925, 2004.

[3] R. Toth, P. Heuberger, and P. Van den Hof, "Asymptotically optimal orthonormal basis functions for LPV system identification," *Automatica*, vol. 45, pp. 1359–70, June 2009.

[4] B. Bamieh and L. Giarre, "Identification of linear parameter varying models," *International Journal of Robust and Nonlinear Control*, vol. 12, pp. 841–853, Jul 2002.

[5] M. Spiridonakos and S. Fassois, "Parametric identification of a time-varying structure based on vector vibration response measurements," *Mechanical Systems and Signal Processing*, vol. 23, no. 6, pp. 2029 – 2048, 2009. Special Issue: Inverse Problems.

[6] H. Garnier and L. Wang, *Identification of Continuous-time Models from Sampled Data*. London: Springer, 2008.

[7] R. Pintelon and J. Schoukens, *System Identification – A frequency domain approach*. IEEE Press, Piscataway, 2001.

[8] J. Lataire and R. Pintelon, "Frequency domain identification of linear, deterministically time-varying systems," in *IFAC - International Federation of Automatic Control*, pp. 11474–11479, 2008.

[9] A. V. Oppenheim, A. S. Willsky, and S. H. Nawab, *Signals & Systems*. New Jersey: Prentice-Hall International, inc., 2nd ed., 1983.

[10] J. Lataire and R. Pintelon, "Frequency domain weighted nonlinear least squares estimation of continuous-time, time-varying systems." Under review for: IET – Control theory and applications, April 2010.

[11] S. Van Huffel and J. Vandewalle, *The total least squares problem: computational aspects and analysis*. Frontiers in Applied Mathematics, USA: SIAM, 1991.

VII. Appendix

A. Origin of the transient term

For $x(t)$, an arbitrary time domain signal with continuous derivatives up till order n, multiplied by a rectangular window of length T, it is easily shown that [7]:

$$\mathcal{L}\left\{\frac{d^n x(t)}{dt^n}\right\} = \int_0^T \frac{d^n}{dt^n} x(t) e^{-st} \mathrm{d}t \tag{21}$$
$$= s^n X(s) + \underbrace{\sum_{r=0}^{n-1} s^r \left(e^{-sT} x^{(n-1-r)}(T\text{-}) - x^{(n-1-r)}(0+)\right)}_{\equiv I_x(s)}$$

with $X(s) = \int_0^T x(t) e^{-st} \mathrm{d}t$, the Laplace Transform of the windowed signal, and $x^{(m)}$ is the mth time derivative of x. This is proven using partial integration. When evaluated at the DFT frequencies $s_k = j\omega_k = \frac{j2\pi k}{T}$, $I_x(s_k)$ is easily shown to be a polynomial in s_k of order $n-1$ (since $\forall k \in \mathbb{Z}$, $e^{-s_k T} = e^{-j2\pi k} = 1$.) Also, the derivative of $I_x(s)$ w.r.t. s remains a polynomial at s_k.

It is well known (see for instance Chapter 9 of [9]) that the Laplace transform of a signal $x(t)$ multiplied by t^p is

$$\mathcal{L}\{t^p x(t)\} = (-1)^p \frac{d^p}{ds^p} \mathcal{L}\{x(t)\} \tag{22}$$

In other words, a multiplication by a monomial of time in the time domain corresponds to a derivative in the Laplace domain. Applying this property to the left hand side of (9) gives

$$\mathcal{L}\left\{t^p \frac{d^n x(t)}{dt^n}\right\} = (-1)^p \frac{d^p}{ds^p}\mathcal{L}\left\{\frac{d^n x(t)}{dt^n}\right\} \tag{23}$$

which, by applying (21) gives the first line of (9).

B. Spectrum of a time monomial

The Laplace transform of a windowed monomial t^p is computed as follows (for $p > 0$ and $s \neq 0$):

$$\begin{aligned}\mathcal{L}\{t^p\} &\equiv \int_0^T t^p e^{-st}\mathrm{d}t \\ &= -\frac{1}{s}\left[t^p e^{-st}\right]_0^T + \frac{p}{s}\underbrace{\int_0^T t^{p-1}e^{-st}\mathrm{d}t}_{=\mathcal{L}\{t^{p-1}\}}\end{aligned} \tag{24}$$

Solving this recursively yields:

$$\mathcal{L}\{t^p\}|_{s=j\omega_k} = -\sum_{n=1}^{p}\frac{1}{(j\omega_k)^n}\frac{p!}{(p-n+1)!}T^{p-n+1} \tag{25}$$

$\mathcal{F}\{t^p\}$ sampled at the DFT frequencies (except at $k = 0$) is thus a sum of hyperbolas of increasing order. For $k = 0$ and $p \geq 0$, we have:

$$\mathcal{F}\{t^p\}|_{s=0} = \int_0^T t^p \mathrm{d}t = \frac{T^{p+1}}{p+1} \tag{26}$$